Published in final edited form as:

Mol Carcinog. 2016 December ; 55(12): 2291–2303. doi:10.1002/mc.22469.

Gene Expression Signatures Associated With Suppression of TRAMP Prostate Carcinogenesis by a Kavalactone-Rich Kava Fraction

Su-Ni Tang[1], **Jinhui Zhang**[1], **Peixin Jiang**[1], **Palika Datta**[1], **Pablo Leitzman**[2], **M. Gerard O'Sullivan**[3], **Cheng Jiang**[1], **Chengguo Xing**[2,**], and **Junxuan Lü**[1,*]

[1]Department of Biomedical Sciences, Texas Tech University Health Sciences Center School of Pharmacy, Amarillo, Texas

[2]Department of Medicinal Chemistry, University of Minnesota College of Pharmacy, Minneapolis, Minnesota

[3]Department of Veterinary Population Medicine and University of Minnesota Masonic Cancer Center Comparative Pathology Shared Resource, College of Veterinary Medicine, St. Paul, Minnesota

Abstract

Kava (*Piper methysticum* Forster) extract and its major kavalactones have been shown to block chemically induced lung tumor initiation in mouse models. Here we evaluated the chemopreventive effect of a kavalactone-rich Kava fraction B (KFB), free of flavokavains, on carcinogenesis in a transgenic adenocarcinoma of mouse prostate (TRAMP) model and characterized the prostate gene expression signatures. Male C57BL/6 TRAMP mice were fed AIN93M diet with or without 0.4% KFB from 8 wk of age. Mice were euthanized at 16 or 28 wk. The growth of the dorsolateral prostate (DLP) lobes in KFB-treated TRAMP mice was inhibited by 66% and 58% at the respective endpoint. Anterior and ventral prostate lobes in KFB-treated TRAMP mice were suppressed by 40% and 49% at 28 wk, respectively. KFB consumption decreased cell proliferation biomarker Ki-67 and epithelial lesion severity in TRAMP DLP, without detectable apoptosis enhancement. Real time qRT-PCR detection of mRNA from DLP at 28 wk showed decreased expression of cell cycle regulatory genes congruent with Ki-67 suppression. Microarray profiling of DLP mRNA indicated that "oncogene-like" genes related to angiogenesis and cell proliferation were suppressed by KFB but tumor suppressor, immunity, muscle/neuro, and metabolism-related genes were upregulated by KFB in both TRAMP and WT DLP. TRAMP mice fed KFB diet developed lower incidence of neuroendocrine carcinomas (NECa) (2 out of 14 mice) than those fed the basal diet (8 out of 14 mice, $\chi^2 = 5.6$, $P < 0.025$).

*Correspondence to: Department of Pharmacology, Penn State Hershey College of Medicine, Hershey, PA 17033. **Correspondence to: Department of Medicinal Chemistry, College of Pharmacy, University of Minnesota, 2231 6th St SE, Minneapolis, MN 55455. Current address of Cheng Jiang and Junxuan Lü is Department of Pharmacology, Pennsylvania State University College of Medicine, Hershey, Pennsylvania.

Conflicts of interest: All authors have no personal or financial conflict of interest and have not entered into any agreement that could interfere with our access to the data on the research or on our ability to analyze the data independently, to prepare and publish articles.

SUPPORTING INFORMATION

Additional supporting information may be found in the online version of this article at the publisher's web-site.

KFB may, therefore, inhibit not only TRAMP DLP epithelial lesions involving multiple molecular pathways, but also NECa.

Keywords

TRAMP; Kava kavalactone rich fraction; prostate epithelial lesions; neuroendocrine carcinoma

INTRODUCTION

Prostate cancer (PCa) is the second leading cause of cancer-death in American men. Chemoprevention by using natural products that modify and intersect the carcinogenesis process in early precancerous stages to prevent or delay cancer has been pursued by us and others as a plausible approach to deal with PCa problem at the root. The transgenic adenocarcinoma of the mouse prostate (TRAMP) model is one of the best characterized and most widely used models in chemoprevention studies since its inception in 1995 [1]. This model was engineered to express simian virus 40 (SV40) early-region tumor T/t antigens in the prostate under the control of rat probasin (PB) promoter [1]. In contrast to the original paradigm of single lineage progression of lesions from mild epithelial hyperplasia, prostatic intraepithelial neoplasia (PIN) to aggressive metastatic poorly differentiated neuroendocrine carcinomas (NECa) [1], it is currently understood that TRAMP mice possess at least two distinct lineages of prostate carcinogenesis [2–4]. One lineage exhibits progressive stages of PIN-like lesions, which were re-named in later studies as “atypical hyperplasia of Tag” (AHTag) because unlike PIN in humans and other mice models they are morphologically unique diffuse lesions and do not develop into invasive carcinoma [2]. The other lineage arises from malignantly transformed progenies of stem-like cells of neuroendocrine origin to develop into the poorly differentiated NECa, without evidence of trans-differentiation from AHTag [2–4]. The epithelial lineage lesions develop in all lobes, especially prominent in the dorsolateral prostate lobes (DLP), whereas the NECa preferentially arises in the smallest ventral prostate (VP) lobes [2,3]. The mouse genetic background profoundly affects the incidence of the NECa: in the C57BL/6 genetic background, the reported incidence rate varied from 20% to 40% [2,3], while in the FVB mouse strain where the TRAMP model initially originated, nearly 100% of the mice develop NECa [5].

Epidemiological studies have suggested that populations with greater consumption of Kava, *Piper methysticum* Forster, had lower age-standardized cancer incidence in the Pacific islands in spite of heavy use of tobacco [6]. Six major kavalactones, namely, kavain, dihydrokavain, methysticin, dihydromethysticin, yangonin, and desmethoxyyangonin, constitute approximately 96% of the total kavalactones in the lipid extract from the Kava rootstock [7]. Cell culture studies have suggested some kavalactones exhibit anti-cancer potential possibly through multiple cellular and molecular signaling pathways [8–10]. We have shown that Kava ethanol extract exerted chemopreventive activity against nicotine-derived nitrosamine ketone (NNK)- and/or benzo[a]pyrene-induced lung tumor initiation in A/J mice [11,12] and chemically induced colon tumorigenesis in the Wistar rats [13]. Furthermore, a kavalactone-rich Kava fraction (KFB) and its dihydromethysticin and

methysticin blocked NNK-induced DNA adduct formation and lung tumor initiation, without liver-damaging side effect [12].

The cross-organ inhibitory activities on carcinogenesis prompted the current study to test the hypothesis that KFB might inhibit the two lineages of prostate carcinogenesis in the TRAMP model. We chose to use the C57BL/6 TRAMP mice in preference to the FVB TRAMP mice due to the attenuated NE-carcinogenesis in the former, permitting the evaluation of impact on the epithelial lineage as well as the NECa lineage. Our data show that KFB supplemented in diet inhibited prostate epithelial proliferation and lesion severity, and reduced the incidence of NECa in TRAMP mice. Immunohistochemistry (IHC) characterization and qRT-PCR gene expression analyses of the TRAMP DLP indicate that KFB inhibited epithelial lesion proliferation without evidence of apoptosis enhancement. Microarray profiling of DLP mRNA indicated that “oncogenelike” genes related to angiogenesis and cell proliferation were suppressed by KFB but many tumor suppressor, immunity, muscle/neuro, and metabolism-related genes were upregulated by KFB in both TRAMP and WT DLP.

MATERIALS AND METHODS

Animal Breeding and Genotyping

The animal use protocols were approved by the Institution Animal Care and Use Committee of Texas Tech University Health Sciences Center (TTUHSC). Male C57BL/6J and female C57BL/6-Tg TRAMP 8247Ng/J mice at the age of 6 wk were purchased from The Jackson Laboratory (Bay Harbor, ME) and subsequently bred in the TTUHSC animal facility at Amarillo. The mice were housed in individually-vented cages with controlled temperature (22–23°C), humidity (55–60%), and a daily 12-h light-dark cycle. Mouse genomic DNA was isolated from ear snips using REDExtract-N-Amp™ Tissue Kit (Sigma-Aldrich Co. LLC., St. Louis, MO) as we described previously [14]. Conventional PCR was performed as described previously [15] with primers obtained from Integrated DNA Technologies, Inc. (Coralville, IA).

Preparation of KFB Diet and Animal Treatments

KFB was isolated from Kava ethanol extract and characterized as previously described [12]. Typically, 1 g of KFB was dissolved in 3 ml of absolute ethanol, mixed with 250 g of Teklad AIN-93M semi-purified powdered diet (Harlan Laboratories, Inc., Indianapolis, IN) and made into moist cookies. Control (i.e., ethanol-supplemented) and KFB-supplemented cookies were freshly made each week. The cookies were air-dried on the bench top and stored at 4°C and were provided to mice twice per week. The level of dietary KFB was chosen based on its lung tumor chemopreventive efficacy in female A/J mice [12]. Male TRAMP mice and their wild type (WT) littermates were assigned at 8 wk of age to AIN-93M control cookies or 0.4% KFB cookies until 16 or 28 wk, unless large tumors in TRAMP mice necessitated earlier euthanasia.

Euthanasia/Necropsy

Blood was taken by cardiac puncture after anesthesia for plasma preparation. At necropsy, the genitourinary (GU) tract including bladder, seminal vesicles, and prostates was removed en bloc and weighed as we described previously [14]. Tumors were dissected and weighed. The prostate lobes from mice without visible tumors were dissected and weighed. Liver, kidney, and other major organs were inspected for health problems and weighed. Mouse genotypes were carefully re-validated by SV40-T antigen (T-Ag) staining of prostate lobes.

Histology and Immunohistochemical (IHC) Staining

Formalin-fixed tumors, prostate lobes, and livers were processed, embedded in paraffin, and routinely stained by H&E. Immunohistochemistry (IHC) for TRAMP carcinogenesis marker proteins were performed as previously reported [3,14,15]. The SV40-T antigen (T-Ag), androgen receptor (AR), and synaptophysin antibodies were purchased from BD Pharmingen (San Diego, CA), EMD Millipore (Billerica, MA), and BD Transduction Laboratories (San Diego, CA), respectively. The secondary antibodies were obtained from Vector Laboratories (Burlingame, CA). Histologic analysis of the livers was performed using light microscopy by an A.C.V.P.-board certified pathologist (M.G. O'S.) under blinded conditions.

Terminal Deoxynucleotidyl Transferase dUTP Nick End Labeling (TUNEL) Assay

Apoptotic cells from tissue sections were detected by the Calbiochem TdT-FragEL DNA Fragmentation Detection Kit (EMD Millipore, Billerica, MA) according to the manufacturer's instructions. In brief, paraffin tissue sections (5-μm thick) were deparaffinized in xylene, rehydrated in ethanol, and digested with 20 μg/ml proteinase K for 20 min. at room temperature. Sections were then incubated with TdT enzyme for 60 min. at 37°C, followed by development with DAB solution and counterstained with methyl green. A dark brown DAB signal signifies positive staining, and shades of blue-green to greenish tan signify a non-reactive cell.

Histopathological Scoring of Prostate Epithelial Lesions

Mouse prostatic tumors or lobes from TRAMP mice were characterized by H&E and T-Ag IHC staining. Prostatic lesions were scored according to our composite scoring scheme modified based on that of Suttie and co-workers [14,16]. In brief, severity of epithelial lesions was divided into five grades: mild lesions as grade I, moderate lesions as grade II, severe lesions as grade III-IV, and adenoma as grade V. The lesion grade was modified by their distribution patterns as focal, multifocal, or diffuse. Therefore, scores for grade I lesions ranged from 1 to 3, and those for grade V ranged from 13 to 15. For each lobe, the most severe lesion and its distribution pattern were used to derive the lesion score.

RNA Isolation and Real-Time Quantitative Reverse Transcription PCR (Real-Time qRT-PCR)

Total RNA was isolated from pooled mouse DLP lobes using the AllPrep DNA/RNA/Protein Mini kit (QIAGEN Inc., Valencia, CA). RNA concentration was determined using the Nano Drop 1000 Spectrophotometer (Thermo Fisher Scientific Inc., Waltham, MA). cDNA was synthesized using the iScript cDNA synthesis kit (Bio-Rad Laboratories, Inc., Hercules, CA)

according to the manufacturer's instructions. Real-time qPCR was performed using the Fast Start Universal SYBR Master with ROX (F. Hoffmann-La Roche Ltd., Basel, Switzerland) on the CFX96 Touch Real-Time PCR Detection Systems (Bio-Rad Laboratories, Inc., Hercules, CA). All reactions were performed in triplicate, and the relative expression of target mRNA in each sample was normalized with that of mean b-actin abundance. The primers were purchased from Integrated DNA Technologies, Inc. (Coralville, IA) and their sequences were listed in Supplement Table S1.

Microarray Analysis of mRNA Expression

mRNA expression profiles were analyzed using Mouse Ref-8 BeadChip expression array (Illumina, Inc., San Diego, CA). All RNA labeling and hybridization was performed at the BioMedical Genomics Center of the University of Minnesota according to protocols specified by the manufacturers. Web-based bioinformatics tools DAVID (The Database for Annotation, Visualization and Integrated Discovery) Bioinformatics Resources version 6.7 (SAIC-Frederick, Inc., Frederick, MD) and IMPaLA (Integrated Molecular Pathway Level Analysis) version 7 (Max-Planck-Gesellschaft, München, Germany) were employed for pathway over-representation and enrichment analyses.

Statistical Analysis

The mean and standard deviation (SD) were calculated for each experimental group. Differences among groups were analyzed by one or two way ANOVA using PRISM statistical analysis software, when the data distribution conformed to normality and homogeneity requirements (GraphPad Software, Inc., La Jolla, CA). For comparisons involving only two groups, Student's *t*-test was used. Significant differences were calculated at $P < 0.05$.

RESULTS

Dietary KFB Consumption Decreased the Incidence of NECa

Enrollment of TRAMP mice and their wild type littermates (WT) into the dietary groups is summarized in Table 1A. Genotypes were confirmed by IHC staining for T-Ag protein in all tumors and prostate lobes (Supplement Figure S1). The incidence of histology- and IHC-verified NECa (see Supplement Figure S1A for characterization of NE marker synaptophysin [SYP], T-Ag, and lack of AR) was one small NECa out of six TRAMP mice fed basal control diet, while none was detected out of eight TRAMP mice in KFB-fed group at 16 wk. In the 28-wk cohorts, the incidence of NECa was decreased from 57% (8 out of 14 TRAMP mice) in control diet group to 14% (2 out of 14) in KFB-fed TRAMP mice ($\chi^2 = 5.6$, $P < 0.025$). Due to the extreme small number of NECa in KFB-fed mice limiting generalizability, we chose not to pursue detailed transcriptomic analyses.

Dietary KFB Consumption Increased Relative Liver Weight Without Affecting Hepatic Integrity

Because the rapid NECa growth can affect the tumor-bearing mice's health and metabolism, we excluded those bearing a NECa for calculation of body and organ weight data to evaluate the health impact of KFB diet consumption. In the 16-wk cohort, KFB diet consumption did

not significantly affect body weight (Figure 1A). In the 28-wk cohorts, both the WT and TRAMP mice on KFB diet gained less weight than those fed the control diet starting at 18 wk (Figure 1B). Once corrected for body weight differences at necropsy, KFB diet consumption increased relative liver weight in both WT and TRAMP mice at 16 and 28 wk (Figure 1C and D, solid bars), but did not influence the relative kidney weight (Figure 1C and D, empty bars). Microscopic evaluation of the livers by A.C.V.P.-board certified pathologist (M.G. O'S.) indicated that there was vacuolar change attributed to glycogen accumulation in both control and treated livers. In addition there was a subtle accentuation of lobular pattern involving the centrilobular (periacinar) area in treated livers that was characterized by a mild to moderate increase in size of the hepatocytes and a subtle eosinophillic granular appearance of the cytoplasm. Measurement of plasma enzyme markers of hepatocyte damage, aspartate transaminase (AST/SGOT), and alanine aminotransferase (ALT/SGPT) showed that KFB did not significantly increase AST or ALT plasma level in both WT and TRAMP mice either by 16 or 28 wk (Table 1B). Therefore, KFB consumption did not appear to impact hepatocyte integrity in either WT or TRAMP mice in spite of increasing relative liver size.

Dietary KFB Consumption Decreased TRAMP Prostate Lobe Growth

We calculated the TRAMP-driven growth of individual prostate lobes over the WT baseline, excluding NE-Ca bearing mice. As expected, the TRAMP DLP underwent the greatest extent of expansion among the different lobes at 16 wk (Figure 2B, column 3 vs. 1) and was inhibited by KFB diet consumption by 66% ($P<0.01$) (Figure 2B, column 4 vs. 3). The continual TRAMP DLP expansion through 28 wk was suppressed by KFB diet by 58% ($P<0.001$) (Figure 2E, column 4 vs. 3). The TRAMP AP lobes expanded only modestly by 16 wk (Figure 2A, column 3 vs. 1) but grew substantially by 28 wk (Figure 2D, column 3 vs. 1) and such growth was suppressed by KFB diet consumption by 40% (Figure 2D, column 4 vs. 3). The VP lobes were smallest compared to AP and DLP, and their modest TRAMP-driven growth was suppressed by KFB by 16 and 28 wk (Figure 2C and F).

KFB Decreased the Severity of Epithelial Lesions in TRAMP Prostate

Staining for T-Ag in the different lobes of TRAMP mice showed ubiquitous expression in the epithelial cells of DLP and VP at both 16 and 28 wk (more than 95% cells positive) (Figure 3A). The AP showed variable and focal T-Ag positive clusters among negative epithelium by 16 wk (not shown) whereas by 28 wk, the staining was mostly positive (Figure 3A). The delayed expression of T-Ag in AP compared to DLP and VP could, therefore, account for the modest increase in TRAMP AP weight over WT baseline at 16-wk endpoint (Figure 2A). As expected of WT mice, IHC staining of epithelial cells did not detect T-Ag in their prostates (Supplement Figure S1B). KFB feeding decreased the complexity and severity of the TRAMP lesions in AP and DLP without affecting T-Ag expression (see examples in Figure 3A). KFB consumption did not cause observable morphological changes in prostate lobes of WT mice (Supplement Figure S1B). The TRAMP VP lobes retained mostly simple epithelial architecture and the morphology was not greatly influenced by KFB diet consumption (Figure 3A).

To quantify the modulation of epithelial lesion severity by KFB diet consumption, we evaluated TRAMP AP, DLP, and VP lobes according to our modified scoring scheme [14]. Briefly, we scored each lobe of TRAMP mice for the most severe epithelial lesion (grade I-V) modified by its distribution pattern as focal, multi-foci, or diffuse (1=focal mild hyperplasia to 15=diffuse adenoma). From 16 to 28 wk, the mean lesion score of AP was 8.4 and 9.7 in TRAMP mice on the basal diet. Dietary KFB consumption significantly decreased the mean lesion score of AP to 3.9 ($P<0.01$) by 16 wk and to 6.4 ($P<0.01$) by 28 wk (Figure 3B). Similarly, KFB also reduced the mean lesion score of DLP from 7.8 in control TRAMP mice to 5.7 ($P<0.05$) by 16wk, from 11.4 to 7.3 ($P<0.01$) by 28 wk, respectively. For TRAMP VP, dietary KFB did not significantly affect the lesion scores at either time point, which remained at the stage of diffuse moderate hyperplasia (Figure 3B). Overall, the growth and severity of epithelial lesions were decreased by KFB in TRAMP DLP and AP lobes.

KFB Inhibited Epithelial Lesion Proliferation in TRAMP Prostate

To probe the cellular processes affected by KFB diet consumption on TRAMP prostate epithelial lesions, we examined prostate tissues for Ki-67 staining as a biomarker for proliferation. The Ki-67 expression levels were decreased in both AP and DLP in TRAMP mice fed KFB diet at 28 wk (Figure 3C). Although nearly 100% of the epithelial cells in VP showed T-Ag positivity (Figure 3A), no more than 5% of them expressed Ki-67 and there was no obvious effect of KFB (Figure 3C). The low proliferative rate in TRAMP VP was consistent with the strong “secretory differentiation” program in this lobe to maintain its glandular architecture and milder histopathology than in the other lobes.

KFB-Treated TRAMP Prostate Lacked Detectable Increase of Apoptosis

DNA fragmentation resulting from apoptosis could be detected by TUNEL assay [17]. TRAMP prostate lobes showed less than 5% of TUNEL-positive cells for mice on control basal diet and KFB diet consumption did not increase TUNEL-positive cells in the epithelial compartments (Supplement Figure S2A). The IHC staining of cleaved caspase 3 did not detect increased apoptotic activation in the three prostate lobes of TRAMP mice treated with KFB diet (Supplement Figure S2B). Therefore, KFB consumption was not likely to induce cellular apoptosis in TRAMP prostates.

Targeted Gene Expression Detection of DLP mRNA by Real-Time qRT-PCR

We analyzed the 28-wk DLP samples because of the clear observable morphological impact of KFB diet consumption and the greater amount of tissue available than 16 wk. Total RNA was isolated from four pooled DLP samples (WT-Basal diet, four mice; WT-KFB diet, four mice; TRAMP-basal diet, five mice; TRAMP-KFB diet, six mice). Profiled genes included proliferation biomarkers (e.g., *Ki-67, Pcna),* AR-downstream genes *(Nkx3,* Probasin *Pbsn,* etc.) and literature-reported and our proteomic-profiled TRAMP-associated cell cycle regulatory genes (Table 2). Compared to WT mice fed control basal diet, real-time qRT-PCR detected significant up-regulations of *Ki-67* (>13-fold) and *Pcna* (>fourfold) in DLP of TRAMP mice fed the basal diet, as well as a number of TRAMP-relevant cyclins (Cyclin E1 *Ccne1,* Cyclin A2 *Ccna2),* protein kinase *(Plk1),* patterning genes *(Ezh2, Hmgb2),* and chromosomal maintenance (e.g., *Mcm2, Mcm6).* In spite of their known function as CDK

inhibitory proteins, P21Cip1 *(Cdkn1a)* and P16Ink4a *(Cdkn2a)* are shown to play crucial roles in accelerated cell proliferation in the TRAMP model [18]. In fact, *Cdkn1a* knockout completely blocks TRAMP carcinogenesis [19]. The much increased transcription of *Cdkn2a* was observed in DLP of TRAMP mice, consistent with the previous findings in TRAMP model [20]. These genes were suppressed by dietary KFB to the extent congruent with the decrease of *Ki-67* mRNA and Ki-67 IHC staining, with the exception of *Mcm6.* Between TRAMP and WT DLP, we did not detect substantial elevation of genes known to be overexpressed in the TRAMP NE-Ca *(Stat3, Sirt2, Rela)* (Table 2), affirming the epithelial lineage specific TRAMP molecular signaling events being analyzed.

Regarding AR signaling axis, we observed 60% increase of TRAMP DLP *Ar* mRNA level vs. WT DLP (Table 2), consistent with the increased AR IHC staining intensity in TRAMP DLPs than in WT DLP (Supplement Figure S3). We observed suppressed expression of AR-regulated genes *Nkx3.1, Tmprss2, Pbsn,* and Cyclin D1 *(Ccnd1)* in the TRAMP DLP versus WT counterpart, as expected from literature reports of attenuated AR differentiation signaling in the epithelial lesions in this model [21,22]. KFB diet did not influence the expression of these genes in absolute abundance in the TRAMP DLP. Taken together, these gene expression data were consistent with an anti-proliferative activity through down regulating TRAMP-driven cell cycle progression machinery by KFB in the epithelial lesions, without evident effect on the AR differentiation signaling axis.

Microarray Profiling of DLP Gene Expression Changes by KFB

To obtain a more global perspective on TRAMP transcriptome affected by KFB diet consumption, we profiled mRNA using Illumina Mouse Ref-8 BeadChip on the same pooled RNA samples. To explore threshold cut-off values for meaningful gene changes by microarray detection, we tested the concordance of microarray signals of the gene panel that we had examined by real-time qRT-PCR (Table 2). Microarray detected the suppressed AR-downstream genes in TRAMP versus WT DLP as did real-time qRT-PCR (e.g., *Nkx3.1, Tmprss2, Pbsn, Ccnd1).* For overexpressed genes in TRAMP DLP over WT DLP baseline, microarray produced near matches on *Mcm6, Mcm2, Hmgb2* with real-time qRT-PCR; whereas it failed to detect *Ki-67, Ccna2,* and *Ccne1.* Microarray underestimated the rest of the genes from two to threefold (e.g., *Pcna, Ezh2)* to more than an order of magnitude that was detectable by real-time qRT-PCR (e.g., *Cdkn2a).* Overall, the microarray platform was less able to detect mRNA changes in TRAMP and WT DLP than real-time qRT-PCR, consistent with our earlier profiling experience with NECa mRNA [23]. Given the underestimation due to inherent limitations of probe design and dynamic range for microarray chip, we examined those genes with either more than 30% decrease or 30% increase of gene expression in TRAMP DLP of mice fed KFB diet versus control basal diet for patterns.

KFB-suppressed genes in DLP

Table 3 shows KFB-suppressed genes, that is, the ratio of expression in TRAMP-KFB diet over TRAMPbasal diet ≤0.7. The vast majority of these genes (24 out of 25) was elevated in TRAMP DLP compared to WT DLP (the ratio of TRAMP-basal diet over WT-basal diet>1.3), consistent with their associations with TRAMP carcinogenesis. Some have known

oncogene properties *(Cyp2b10, Sdcbp2, Bst2, Ctgf, Sprr1a),* others are related to cell cycle and proliferation *(Oas1g, Dnase2b),* angiogenesis (*Ang*, *Angptl7, Rnase4),* extracellular matrix and proteases *(Expi, Ctse, Usp18),* chemokine/cytokines *(Ccl21c, Ccl21a, Cxcl14, Mdk),* and a few genes were immunomodulatory *(H2-Q8, H2-Ab1, Cd8b1, Defcr20)* (Table 3). The KFB-suppressed genes were mostly specific to the TRAMP DLP because only three of these genes (i.e., *Bst2*, *Ang*, *Svs3a)* were also suppressed by KFB in the WT DLP (Table 3). Therefore, most of these KFB-suppressed genes were likely relevant to the attenuation of TRAMP epithelial lesion growth and progression.

KFB-induced genes in DLP

Table 4 shows KFB-induced genes, i.e., the ratio of TRAMP DLP-KFB diet over TRAMP DLP-basal diet ≥1.3. Some of these genes in the TRAMP DLP were decreased (TRAMP/WT ratio<0.7), suggestive of "tumor suppressor-like" functions. Indeed, a few of them have recognized tumor suppressor functions (e.g., *Gsta3, Cdo1, Ndn, Serpina1f, Wfdc10).* Other major categories included immunity *(Cfd, Cuzd1, Defb42, Defb43, Defb28, Defb11, Xlr4a),* neuro/brain-related signatures *(Mfsd2, Zcchc18, Sult4a1, Sncg, Vstm2l, Rtn1, Klc1, Bex4, Pvalb),* and many genes involved in metabolic processes, muscle, plus a few genes in the PPARγ pathway. Most of these genes were either moderately lowered in TRAMP DLP than in WT DLP or were not decreased at all. Their induction by KFB diet consumption occurred not only in TRAMP DLP but also in WT DLP. The mRNA induction trend for *Defb42, Lpl,* and *Atp2a1* was confirmed by real-time qRT-PCR (data not shown). Two genes coding for prostate secretory proteins *(Crisp1, Vpp1)* were much lowered in TRAMP DLP than WT DLP. They were partially restored in the TRAMP DLP in mice on the KFB diet. Overall, KFB diet consumption induced genes related to tumor suppressor functions, immunity enhancement, metabolism, and muscle features that suggested a restoration of weakened barriers not only in TRAMP lesions and their microenvironments but also in the normal wild type prostate tissues.

DISCUSSION

Whereas other researchers have endeavored to evaluate the anti-cancer potential of Kava flavokavains against various types of prostate and bladder cancer cells and xenograft models [24,25], we believe that the present study represents the first to determine the in vivo efficacy of kavalactone-rich KFB that was free of the "hepatotoxic" flavokavains in a transgenic primary carcinogenesis model of prostate cancer. We obtained experimental evidence that KFB inhibited epithelial lesions, most dramatically in DLP (Figures 2 and 3), and decreased the incidence of NECa (Table 1). Because chemoprevention of prostate cancer is deemed most impactful by targeting precancerous epithelial lesions through blocking or delaying their progression to carcinomas, we focused our cellular and molecular analyses on changes in TRAMP epithelial lesions, especially those in the DLP. Our data supported an anti-proliferative action on the epithelial lesions as a likely effector cellular process (Figure 3C). However, we detected no apoptosis enhancement in these KFB treated lesions at termination of experiment (Supplement Figure S2), unless the sampling time points missed the apoptosis window. Real-time qRT-PCR targeted analysis of a panel of genes provided

molecular correlates of the anti-proliferative action and confirmation of epithelial lineage specificity at a molecular level (Table 2).

In spite of limitations of the microarray profiling platform, our analyses of the DLP transcriptome changes provided a glimpse into the multitudes of molecular pathways for which FKB consumption had exerted effects. They included suppression of oncogene-like genes involved in cell cycle dysregulation, proliferation, angiogenesis, and invasiveness (Table 3) and induction of many genes of "tumor suppressor" functions, prostate functional differentiation, immunity enhancement, neuro-brain and muscle signatures, and various metabolism pathways that appeared to be more general in both TRAMP and WT DLP (Table 4). Future efforts will need to address cause-effect relationships of these gene changes to the efficacy outcome.

The body weight suppression and liver enlargement (hepatomegaly) observed in this study (Figure 1) should be interpreted with care. After the mice were fed KFB diet for a prolonged period of time (more than 8 wk), they exhibited decreased weight gain in both TRAMP and WT mice. One possible explanation is that Kava extract has been shown as an appetite suppressant through its tranquilizing effect on stomach motility [26]. In spite of the greater relative liver weight normalized to body weight in the KFB-fed mice (Figure 1C and D), plasma enzyme markers of hepatocyte integrity were not adversely affected by KFB (Table 1B). Therefore, the hepatomegaly was likely an adaptive response to metabolize KFB chemicals and distinct from the hepatotoxicity suspected of Kava products. The alleged safety issues might have resulted from inappropriate causality—assessment approaches [27], improper preparation of Kava raw material [28], and fragmented regulatory standards of agencies and manufacturers [29]. Indeed, Xing lab has documented that flavokavains (absent in KFB), but not kavalactones (enriched in KFB), exhibit synthetic hepatotoxicity with the pain killer drug acetoaminophen (Tylenol) in mice [30].

In summary, KFB diet consumption suppressed the growth of TRAMP epithelial lesions and modified a spectrum of genes in the TRAMP DLP on the one hand, and decreased the incidence of NECa on the other. KFB may be a promising natural product modality for prostate cancer lesion intervention in addition to its impressive blocking of lung tumor initiation by tobacco chemicals. Further work will aim to elucidate whether the chemical species in KFB for prostate lesion chemoprevention will overlap with those as lung initiation blockers and to validate the responsible molecular target(s) and cellular processes. In terms of extrapolation of the murine efficacious dose for humans, the daily consumption in the mice in the current study amounted to 480 mg KFB per kg body (assuming 3 g diet consumed per mouse of 25 g weight). By allometric conversion with a factor of 12 [31], for an adult human of 60 kg, the daily intake is estimated to be 2.4 g of KFB, easily manageable in five 500-mg capsules.

Supplementary Material

Refer to Web version on PubMed Central for supplementary material.

ACKNOWLEDGMENT

The authors thank TTUHSC Animal care staff for excellent assistance with mouse breeding and care.

Grant sponsor: National Center for Complementary and Integrative Health (NCCIH); Grant number: R01AT007395; Grant sponsor: National Cancer Institute; Grant numbers: R01 CA136953; R01 CA142649; R01 CA193278

Abbreviations

AP	anterior prostate
DLP	dorsolateral prostate
KFB	Kava fraction B
NECa	neuroendocrine carcinoma
TRAMP	transgenic adenocarcinoma of mouse prostate
VP	ventral prostate

REFERENCES

1. Greenberg NM, DeMayo F, Finegold MJ, et al. Prostate cancer in a transgenic mouse. Proc Nat Acad Sci USA 1995;92:3439–3443. [PubMed: 7724580]
2. Chiaverotti T, Couto SS, Donjacour A, et al. Dissociation of epithelial and neuroendocrine carcinoma lineages in the transgenic adenocarcinoma of mouse prostate model of prostate cancer. Am J Pathol 2008;172:236–246. [PubMed: 18156212]
3. Wang L, Zhang J, Zhang Y, et al. Lobe-specific lineages of carcinogenesis in the transgenic adenocarcinoma of mouse prostate and their responses to chemopreventive selenium. Prostate 2011;71:1429–1440. [PubMed: 21360561]
4. Huss WJ, Gray DR, Tavakoli K, et al. Origin of androgen-insensitive poorly differentiated tumors in the transgenic adenocarcinoma of mouse prostate model. Neoplasia 2007;9:938–950. [PubMed: 18030362]
5. Gingrich JR, Barrios RJ, Foster BA, Greenberg NM. Pathologic progression of autochthonous prostate cancer in the TRAMP model. Prostate Cancer P D 1999;2:70.
6. Steiner GG. The correlation between cancer incidence and kava consumption. Hawaii Med J 2000;59:420–422. [PubMed: 11149250]
7. Lebot V, Lévesque J. The origin and distribution of kava (Piper methysticum Forst. f., Piperaceae): A phytochemical approach. Allertonia 1989;5:223–281.
8. Hashimoto T, Suganuma M, Fujiki H, Yamada M, Kohno T, Asakawa Y. Isolation and synthesis of TNF-alpha release inhibitors from Fijian kawa (Piper methysticum). Phytomedicine: Int J Phytotherap Phytopharmacol 2003;10:309–317.
9. Tabudravu JN, Jaspars M. Anticancer activities of constituents of kava (Piper methysticum). South Pac J Nat Appl Sci 2005;23:26–29.
10. Folmer F, Blasius R, Morceau F, et al. Inhibition of TNFalpha-induced activation of nuclear factor kappaB by kava (Piper methysticum) derivatives. Biochem Pharmacol 2006;71:1206–1218. [PubMed: 16464438]
11. Johnson TE, Kassie F, O'Sullivan MG, et al. Chemopreventive effect of kava on 4-(methylnitrosamino)-1-(3-pyridyl)-1-butanone plus benzo[a]pyrene-induced lung tumorigenesis in A/ J mice. Cancer Prevent Res 2008;1:430–438.
12. Narayanapillai SC, Balbo S, Leitzman P, et al. Dihydromethysticin (DHM) from kava blocks tobacco carcinogen 4-(methylnitrosamino)-1-(3-pyridyl)-1-butanone(NNK)-induced lung

tumorigenesis and differentially reduces DNA damage in A/J mice. Carcinogenesis 2014;35:2365–2372. [PubMed: 25053626]

13. Triolet J, Shaik AA, Gallaher DD, O'Sullivan MG, Xing C. Reduction in colon cancer risk by consumption of kava or kava fractions in carcinogen-treated rats. Nutr Cancer 2012;64: 838–846. [PubMed: 22693990]
14. Tang SN, Zhang J, Wu W, et al. Chemopreventive effects of Korean Angelica vs. its major pyranocoumarins on two lineages of transgenic adenocarcinoma of mouse prostate carcinogenesis. Cancer Prev Res (Phila) 2015;8:835–844. [PubMed: 26116406]
15. Wang L, Bonorden MJL, Li G-x, et al. Methyl-selenium compounds inhibit prostate carcinogenesis in the transgenic adenocarcinoma of mouse prostate model with survival benefit. Cancer Preven Res 2009;2:484–495.
16. Suttie A, Nyska A, Haseman JK, Moser GJ, Hackett TR, Goldsworthy TL. A grading scheme for the assessment of proliferative lesions of the mouse prostate in the TRAMP model. Toxicol Pathol 2003;31:31–38. [PubMed: 12597447]
17. Negoescu A, Guillermet C, Lorimier P, Brambilla E, Labat-Moleur F. Importance of DNA fragmentation in apoptosis with regard to TUNEL specificity. Biomed Pharmacotherap 1998;52:252–258.
18. Maddison LA, Huss WJ, Barrios RM, Greenberg NM. Differential expression of cell cycle regulatory molecules and evidence for a "cyclin switch" during progression of prostate cancer. Prostate 2004;58:335–344. [PubMed: 14968434]
19. Jain A, Raina K, Agarwal R. Deletion of p21/Cdkn1a confers protective effect against prostate tumorigenesis in transgenic adenocarcinoma of the mouse prostate model. Cell Cycle 2013;12:1598–1604. [PubMed: 23624841]
20. Morey SR, Smiraglia DJ, James SR, et al. DNA methylation pathway alterations in an autochthonous murine model of prostate cancer. Cancer Res 2006;66:11659–11667. [PubMed: 17178860]
21. Bethel CR, Bieberich CJ. Loss of Nkx3.1 expression in the transgenic adenocarcinoma of mouse prostate model. Prostate 2007;67:1740–1750. [PubMed: 17929276]
22. Zhang J, Wang L, Zhang Y, Li L, Higgins L, Lü J. Lobe-specific proteome changes in the dorsal-lateral and ventral prostate of TRAMP mice versus wild-type mice. Proteomics 2011;11:2542–2549. [PubMed: 21598396]
23. Zhang J, Wang L, Zhang Y, et al. Chemopreventive effect of Korean Angelica root extract on TRAMP carcinogenesis and integrative "omic" profiling of affected neuroendocrine carcinomas. Mol Carcinogen 2014.
24. Zi X, Simoneau AR. Flavokawain A, a novel chalcone from kava extract, induces apoptosis in bladder cancer cells by involvement of bax protein-dependent and mitochondria-dependent apoptotic pathway and suppresses tumor growth in mice. Cancer Res 2005;65:3479–3486. [PubMed: 15833884]
25. Li X, Liu Z, Xu X, et al. Kava components down-regulate expression of ar and ar splice variants and reduce growth in patient-derived prostate cancer xenografts in mice. PLoS ONE 2012;7:e31213. [PubMed: 22347450]
26. Lindstrom M Spitting on Tanna. Oceania 1980;50:228–234.
27. Stickel F, Baumüller H-M, Seitz K, et al. Hepatitis induced by Kava (Piper methysticum rhizoma). J Hepatol 2003;39:62–67. [PubMed: 12821045]
28. Lebot V The quality of kava consumed in the South Pacific. HerbalGram 2006;71:34–37.
29. Sarris J, LaPorte E, Schweitzer I. Kava: A comprehensive review of efficacy, safety, and psychopharmacology. Aust NZJ Psychiatry 2011;45:27–35.
30. Narayanapillai SC, Leitzman P, O'Sullivan MG, Xing C. Flavokawains A and B in kava, not dihydromethysticin, potentiate acetaminophen-induced hepatotoxicity in C57BL/6 mice. Chem Res Toxicol 2014;27:1871–1876. [PubMed: 25185080]
31. Sharma V, McNeill JH. To scale or not to scale: The principles of dose extrapolation. Brit J Pharmacol 2009;157:907–921. [PubMed: 19508398]

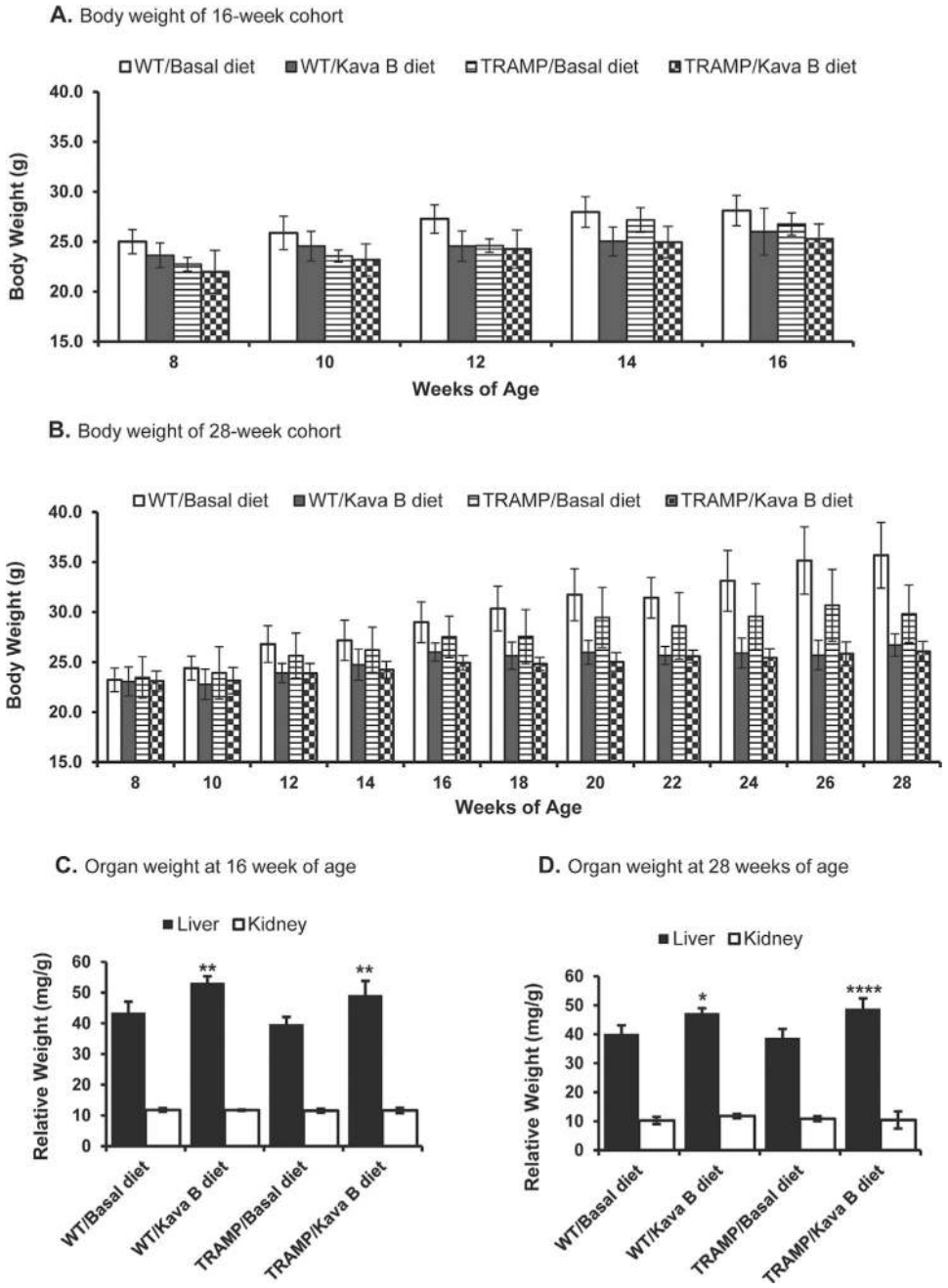

Figure 1.

Effects of KFB diet consumption on body weight and select organ weight of TRAMP and WT mice. Mice bearing NECa were excluded. (A) Body weight of 16-wk cohorts; (B) body weight of 28-wk cohorts; (C) relative organ weight by 16 wk; and (D) relative organ weight by 28 wk. Relative liver and kidney weights (mg/g) are normalized by body weight. Number of mice: 16 wk, WT/Basal control diet, *n*=5; WT/Kava KFB diet, *n*=3; TRAMP/Basal control diet, *n*=5; and TRAMP/Kava KFB diet, *n*=8, respectively; 28 wk, WT/Basal control diet, *n*=4; WT/Kava KFB diet, *n*=4; TRAMP/Basal control diet, *n*=6; and TRAMP/Kava

KFB diet, n=12, respectively. Mean±SD, one-way ANOVA followed by the Dunnett's post hoc test, *: P<0.05; **: P<0.01, ***: P<0.001, ****: P<0.0001.

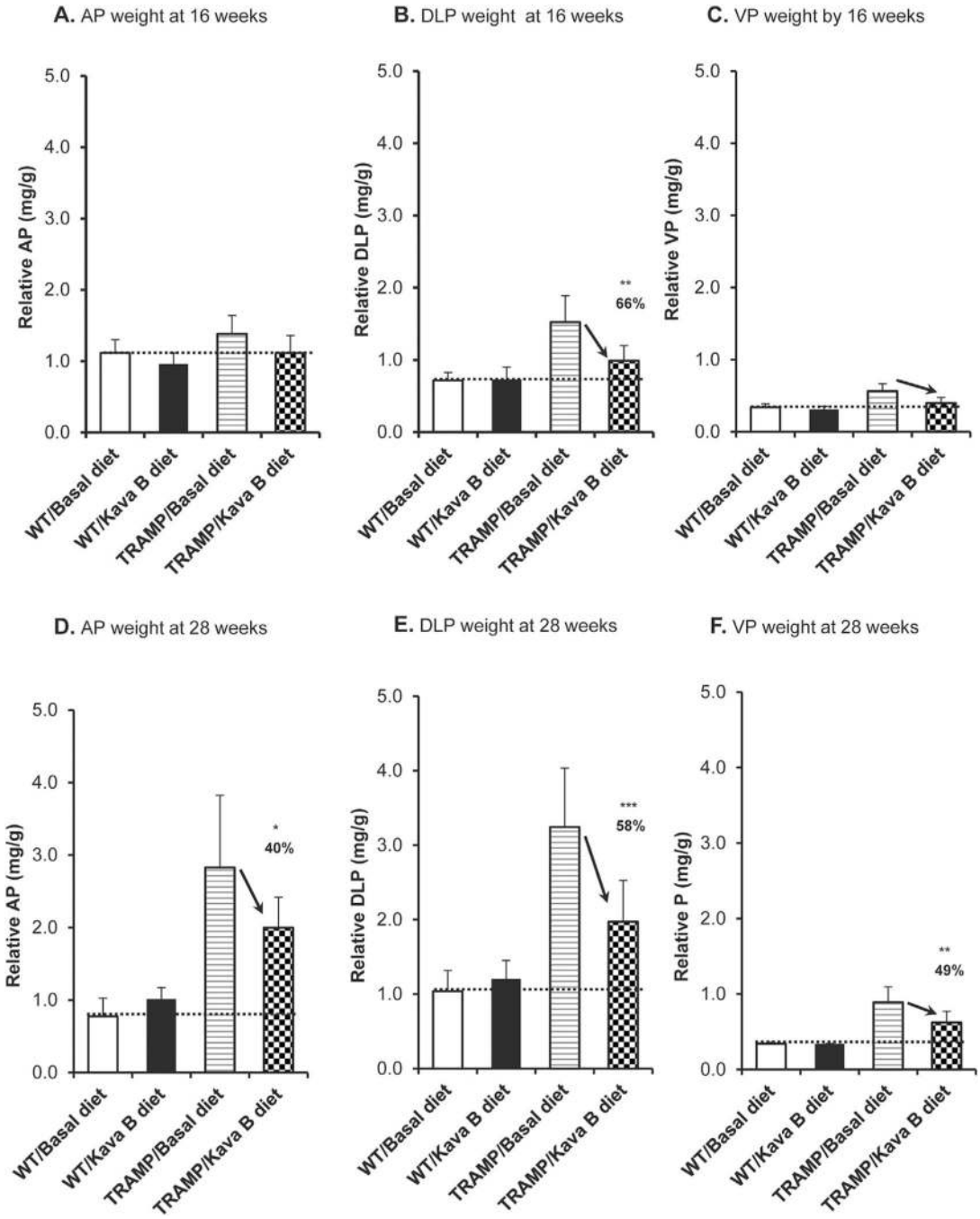

Figure 2.

Effects of KFB diet consumption on the prostatic lobe weight of TRAMP and WT mice. TRAMP mice bearing NE-Ca were excluded. (A) Relative anterior prostate AP weight by 16wk; (B) relative dorsal-lateral prostate DLP weight by 16 wk; (C) relative ventral prostate VP weight by 16 wk; (D) relative AP weight by 28 wk; (E) relative DLP weight by 28 wk; (F) relative VP weight by 28 wk. Relative weights (mg/g) were normalized by the corresponding body weight. Dashed line indicates the WT baseline; % indicates percentage decrease of the expansion in KFB-treated TRAMP mice. Animal numbers: by 16 wk, WT/

Basal control diet, n=5; WT/Kava KFB diet, n=3; TRAMP/Basal control diet, n=5; and TRAMP/Kava KFB diet, n=8, respectively; by 28 wk, WT/Basal control diet, n=4; WT/Kava KFB diet, n=4; TRAMP/Basal control diet, n=6; and TRAMP/Kava KFB diet, n=12, respectively. Mean±SD, one-way ANOVA followed by the Dunnett post hoc test, *: P<0.05; **: P<0.01, ***: P<0.001.

A. T-Ag IHC in TRAMP prostatic lobes at 28 weeks of age

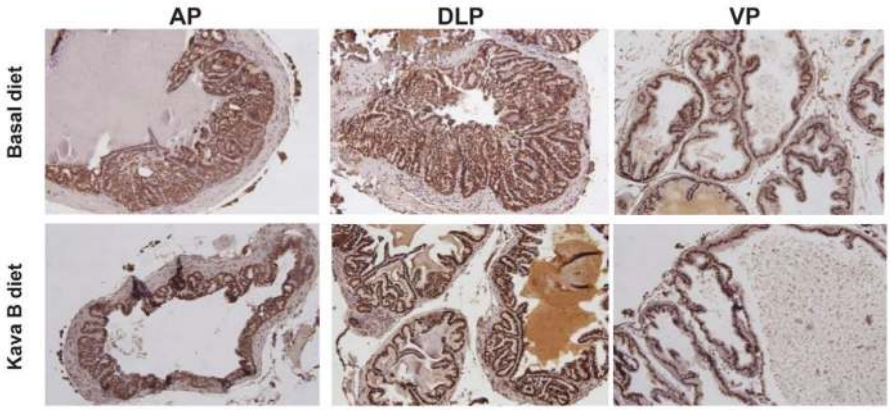

B. Mean score of TRAMP prostatic epithelial lesions

Age	Treatment	Lesion score		
		AP	DLP	VP
16 weeks	Basal diet	8.4±1.5	7.8±2.4	7.6±0.5
	Kava B diet	3.9±2.7**	5.7±1.3*	6.3±1.8
28 weeks	Basal diet	9.7±1.6	11.4±2.9	6.6±1.9
	Kava B diet	6.4±2.6**	7.3±2.3**	6.1±1.8

C. Ki-67 IHC in TRAMP prostatic lobes at 28 weeks of age

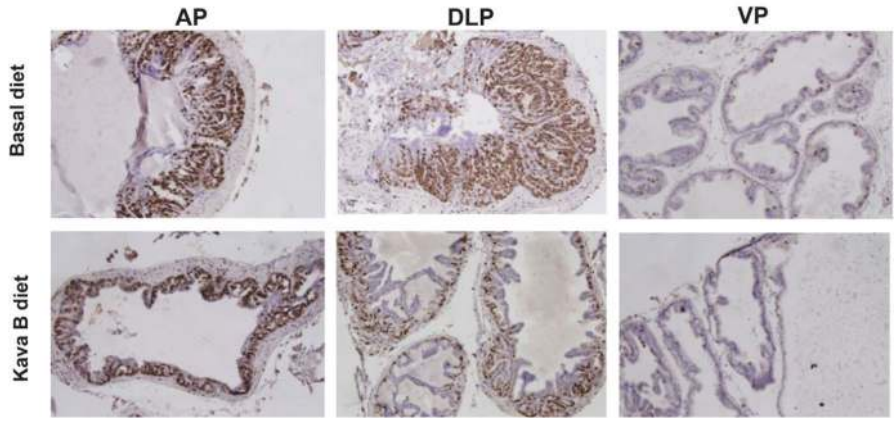

Figure 3.

Effects of KFB diet consumption on SV40-T antigen (T-Ag) expression, lesion severity, and Ki-67 expression in TRAMP mice. (A) Representative photomicrograph of the immunohistochemical analysis of T-Ag expression in TRAMP prostatic lobes (28 wk). The epithelial lesions show T-Ag + nuclei. (B) Mean score of TRAMP prostatic epithelial lesions. The most advanced lesion from each mouse prostatic lobe was scored according to severity and distribution pattern using sections stained with T-Ag. Sections with NE-lesions or without prostatic glands are not included. (C) Representative photomicrograph images of the immunohistochemical analysis of Ki-67 expression in TRAMP prostatic lobes (28 wk). Magnification, 200×. Animal number: by 16 wk, TRAMP/Basal control diet, AP *n*=5, DLP *n*=5, VP *n*=5; TRAMP/Kava KFB diet, AP *n*=8, DLP *n*=8,VP *n*=8; by 28 wk, TRAMP/

Basal control diet, AP n=6, DLP n=5, VP n=5; TRAMP/Kava KFB diet, AP n=11, DLP n=12, VP n=12. Mean±SD, Student's t-test, *: P<0.05; **: P<0.01.

Table 1.

Effects of Kava Fraction B Diet Consumption on the Incidence of TRAMP Mice With NECa and Plasma Enzyme Biomarkers of Liver Integrity

A. The distribution of TRAMP mice with prostate lesions of different lineages.

Age	Genotype/treatment	TRAMP mice enrolled	Mice with only epithelial lesions	Mice with NE tumor (incidence %)
16 wk	TRAMP/basal diet	6	5	1 (16.7)
	TRAMP/Kava B diet	8	8	0 (0)
28 wk	TRAMP/basal diet	14	6	8 (57.1)[a]
	TRAMP/Kava B diet	14	12	2 (14.3)[a]

B. Plasma enzyme biomarkers of liver integrity (excluding NECa bearing mice)

Age	Genotype/treatment	ALT (U/L)	AST (U/L)	n
16 wk	WT/basal diet	36 ± 35	132 ± 57	5
	WT/Kava B diet	27 ± 4	136 ± 22	3
	TRAMP/basal diet	17 ± 2	113 ± 49	6
	TRAMP/Kava B diet	25 ± 9	150 ± 71	8
28 wk	WT/basal diet	24 ± 4	132 ± 35	4
	WT/Kava B diet	20 ± 2	112 ± 31	4
	TRAMP/basal diet	13 ± 2	75 ± 25	6
	TRAMP/Kava B diet	21 5	107 ± 46	12

[a]Chi-square test, $\chi^2 = 5.6$, $P<0.025$.

Mol Carcinog. Author manuscript; available in PMC 2019 May 15.

Table 2.

Effects of Kava Fraction B Diet Consumption on DLP mRNA Expression in 28-wk-Old-Mice: Real Time qRT-PCR and Microarray Data Comparison

	By real time qRT-PCR			By microarray		
	Relative to WT (basal diet) as 1			Relative to WT (basal diet) as 1		
Gene	**WT (Kava)**	**TRAMP (Basal)**	**TRAMP (Kava)**	**WT (Kava)**	**TRAMP (Basal)**	**TRAMP (Kava)**
Ki67	1.31	13.67	11.36	1.02	1.08	1.02
Pcna	1.02	4.86	3.66	0.87	2.03	2.26
Cdkn2a (P16Ink4a)	2.19	216.2	138.9	0.92	5.39	4.06
Ccne1	2.17	35.06	20.46	0.89	1.11	1.19
Plk1	2.48	18.50	11.52	0.90	2.91	2.16
Ccna2	1.07	14.05	9.83	0.93	1.14	1.13
Cdknla (P21Cip1)	1.71	8.02	4.39	1.20	1.68	1.44
Mcm6	1.02	8.71	8.56	0.97	8.21	7.83
Mcm2	1.07	5.21	4.34	0.92	4.41	4.02
Hmgb2	1.22	4.81	3.33	1.09	3.51	3.27
Ezh2	1.26	4.71	3.85	0.96	2.40	2.50
Stat3	1.18	1.75	1.37	0.92	0.92	1.01
Sirt2	1.16	1.27	0.99	0.98	0.84	0.83
Rela	1.14	1.26	1.11	0.98	1.18	1.20
Ar	1.07	1.60	1.41	1.01	1.09	1.26
Ccnd1	0.96	0.58	0.52	0.99	0.35	0.46
Nkx3.1	0.88	0.44	0.46	0.68	0.41	0.40
Tmprss2	0.71	0.43	0.32	0.70	0.33	0.31
Pbsn	0.76	0.01	0.03	0.72	0.03	0.04

Mol Carcinog. Author manuscript; available in PMC 2019 May 15.

Table 3.

Kava Fraction B-Suppressed Genes

Symbol	Gene definition	TRAMP mice (Kava/basal)	WT mice (Kava/basal)	TRAMP/WT (basal diet)	Functional category
Cyp2b10	Cytochrome P450, family 2, subfamily b, polypeptide 10	0.58	1.29	3.11	Oncogenic, carcinogen activation
Sdcbp2	Syndecan binding protein 2	0.66	1.11	2.70	Oncogenic, cell signaling
Sprr1a	Small proline-rich protein 1A	0.59	1.47	1.67	Oncogenic, STAT3 driven
Bst2	Bone marrow stromal cell antigen 2	0.65	0.62	1.54	Oncogenic, expressed in cancers
Ctgf	Connective tissue growth factor	0.70	1.12	1.39	Oncogenic, growth factor
Oas1g	2'−5' oligoadenylate synthetase 1G	0.67	1.10	5.27	Proliferation, nucleotide
Dnase2b	Deoxyribonuclease II beta	0.64	1.05	2.58	Proliferation, DNA replication
Rnase4	Ribonuclease 4	0.69	0.80	2.72	Angiogenesis, angiogenin family
Ang	Angiogenin, ribonuclease, RNase A family, 5	0.70	0.65	1.68	Angiogenesis
Angptl7	Angiopoietin-like 7	0.66	0.81	1.30	Angiogenesis
Svs3a	Seminal vesicle secretion 3A	0.70	0.61	9.21	Prostate epithelial product
Usp18	Ubiquitin specific peptidase 18	0.55	1.03	3.69	Protease
Ctse	Cathepsin E	0.51	1.24	3.60	Protease
Expi	Extracellular proteinase inhibitor	0.54	1.12	1.97	Protease inhibitor
Kera	Keratocan	0.65	0.92	1.41	Extracellular matrix
Ccl21c	Chemokine (C-C motif) ligand 21C	0.70	1.08	1.93	Chemokine
Ccl21a	Chemokine (C-C motif) ligand 21A	0.70	1.24	1.92	Chemokine
Cxcl14	Chemokine (C-X-C motif) ligand 14	0.67	0.96	1.25	Chemokine
Isg15	ISG15 ubiquitin-like modifier	0.69	1.20	3.93	Cytokine, immune evasion
Mdk	Midkine, transcript variant 3	0.69	1.06	1.85	Cytokine
H2-Q8	Histocompatibility 2, Q region locus 8	0.58	1.29	3.78	Immunomodulatory
H2-Ab1	Histocompatibility 2, class II antigen A, beta 1	0.70	1.17	1.76	Immunomodulatory
Cd8b1	CD8 antigen, beta chain 1	0.69	0.88	1.41	Immunomodulatory
Defcr20	Defensin related cryptdin 20	0.67	1.09	1.55	Immunomodulatory
Slamf9	SLAM family member 9	0.69	0.85	1.45	Immunomodulatory

Table 4.

Kava Fraction B-Induced Genes

Symbol	Gene definition	TRAMP mice(Kava/basal)	WT mice (Kava/basal)	TRAMP/WT (basal diet)	Functional category
Gsta3	Glutathione s-transferase, alpha 3, transcript variant 2	1.85	1.38	0.29	Tumor suppressor, phase II de-tox enzyme
Cdo1	Cysteine dioxygenase 1, cytosolic	1.58	0.97	0.32	Tumor suppressor, methylation inactivation
Ndn	Necdin	1.52	1.49	0.49	Tumor supressor, inhibit proliferation
Vip	Vasoactive intestinal polypeptide	1.60	1.70	0.52	Tumor suppressor, anti-inflammatory
Cyp2e1	Cytochrome P450, family 2, subfamily e, polypeptide 1	4.60	7.62	0.68	Tumor suppressor, phase I drug metabolism
Hp	Haptoglobin	1.73	2.64	0.88	Tumor suppressor, anti-inflammatary
Serpina1f	Serine (or cysteine) peptidase inhibitor, clade A, member 1f	2.11	1.42	0.31	Tumor suppressor, protease inhibitor
Wfdc10	WAP four-disulfide core domain 10	1.46	1.16	0.30	Tumor suppressor, protease inhibitor
Crisp1	Cysteine-rich secretory protein 1	1.66	1.20	0.27	Prostate function
Vpp1	Ventral prostate predominant 1	1.59	1.08	0.24	Prostate function
Cuzd1	CUB and zona pellucida-like domains	1.30	0.96	0.27	Immunity
Defb11	Defensin beta 11	1.40	1.10	0.35	Immunity
Defb28	Defensin beta 28	1.58	0.98	0.29	Immunity
Defb42	Defensin beta 42	1.98	1.09	0.21	Immunity
Defb43	Defensin beta 43	1.74	1.56	0.38	Immunity
Mmd	Monocyte to macrophage differentiation-associated	1.62	1.62	0.59	Immunity
Cfd	Complement factor D (adipsin)	5.88	7.95	0.61	Immunity
Xlr4a	X-linked lymphocyte-regulated 4A	2.41	1.74	0.85	Immunity
Mfsd2	Major facilitator superfamily domain containing 2	1.51	1.38	0.29	Neuro, brain circadian rhythm
Zcchc18	Zinc finger, CCHC domain containing 18, transcript variant 3	1.53	1.24	0.37	Neuro protein
Sult4a1	Sulfotransferase family 4A, member 1	1.63	1.28	0.38	Neuro, brain, estrogen stimulated
Sncg	Synuclein, gamma	1.61	1.32	0.41	Neuro protein
Vstm2l	V-set and transmembrane domain containing 2-like	1.58	1.30	0.41	Neuro, secretory antagonist to humanin
Rtn1	Reticulon 1, transcript variant 2	1.78	1.34	0.43	Neuro protein
Klc1	Kinesin light chain 1, transcript variant a	1.56	1.30	0.45	Neuro, brain, intracellular traffic
Bex4	Brain expressed gene 4	1.62	1.06	0.56	Neuro, brain
Pvalb	Parvalbumin	1.49	1.83	0.58	Neuro, Ca(2+)- binding protein

Symbol	Gene definition	TRAMP mice(Kava/basal)	WT mice (Kava/basal)	TRAMP/WT (basal diet)	Functional category
Eef1a2	Eukaryotic translation elongation factor 1 alpha 2	1.57	1.44	0.43	Metabolism, protein synthesis
Rpl3l	Ribosomal protein L3-like	1.41	1.48	0.58	Metabolism, protein synthesis
Pygl	Liver glycogen phosphorylase	1.77	1.44	0.51	Metabolism, glucose
Gldc	Glycine decarboxylase	1.51	1.44	0.47	Metabolism, intermediate
Pgam2	Phosphoglycerate mutase 2	1.39	1.97	0.66	Metabolism, glycolysis
Lpl	Lipoprotein lipase	2.53	2.73	0.67	Metabolism, lipid
Retnla	Resistin like alpha	1.76	1.71	0.59	Metabolism, lipid
Akr1b7	Aldo-keto reductase family 1, member B7	1.72	1.21	0.42	Metabolism, lipid
Ces3	Carboxylesterase 3	1.63	1.36	0.43	Metabolism, lipid
Apoc1	Apolipoprotein C-I	1.51	1.52	0.68	Metabolism, lipid
Thrsp	Thyroid hormone responsive SPOT14 homolog	2.32	2.37	0.81	Metabolism, lipid
Acaca	Acetyl-coenzyme A carboxylase alpha	1.56	1.38	0.85	Metabolism, lipid
Cidea	Cell death-inducing DNA fragmentation factor, alpha subunit-like effector A	2.04	1.95	0.90	Metabolism, lipid, adiposity
Lrg1	Leucine-rich alpha-2-glycoprotein 1	1.73	1.55	0.93	Metabolism, lipid
Scd1	Stearoyl-coenzyme A desaturase 1	1.82	2.82	0.98	Metabolism, lipid
Cox6a2	Cytochrome c oxidase subunit Via polypeptide 2	1.51	1.81	0.58	Metabolism, mito oxphos
Cox7a1	Cytochrome c oxidase subunit Vila polypeptide 1	1.33	1.52	0.83	Metabolism, mito oxphos
Cox8b	Cytochrome c oxidase, subunit Vlllb	2.05	2.16	0.83	Metabolism, mito oxphos
Slco2a1	Solute carrier organic anion transporter family, member 2a1	1.72	1.04	0.29	Ion transport
Scara5	Scavenger receptor class A, member 5 (putative)	1.78	1.71	0.63	Ion transport, non-Trf iron
Trf	Transferrin	1.88	2.73	0.68	Ion transport
Tnni2	Troponin I, skeletal, fast 2	1.76	1.90	0.54	Muscle
Atp2a1	ATPase, Ca++ transporting, cardiac muscle, fast twitch 1	1.62	1.75	0.57	Muscle
Mb	Myoglobin	1.56	1.68	0.62	Muscle
Ttn	Titin, transcript variant N2-B	1.53	1.57	0.62	Muscle
Tnnc2	Troponin C2, fast	1.51	1.56	0.61	Muscle
Tpm2	Tropomyosin 2, beta	1.49	1.83	0.61	Muscle
Actn3	Actinin alpha 3	1.40	1.61	0.62	Muscle
Tnnt3	Troponin T3, skeletal, fast	1.30	1.83	0.70	Muscle
Myl1	Myosin, light polypeptide 1	1.63	1.82	0.62	Muscle

Symbol	Gene definition	TRAMP mice(Kava/basal)	WT mice (Kava/basal)	TRAMP/WT (basal diet)	Functional category
Mylpf	Myosin light chain, phosphorylatable, fast skeletal muscle	1.54	1.75	0.74	
Myh1	Myosin, heavy polypeptide 1, skeletal muscle, adult	1.40	2.06	0.73	Muscle
Myh8	Myosin, heavy polypeptide 8, skeletal muscle, perinatal	1.80	2.58	0.76	Muscle
Mybpc2	Myosin binding protein C, fast-type	1.39	1.66	0.85	Muscle
Adipoq	Adiponectin, C1Q and collagen domain containing	3.21	5.57	0.74	PPARγ signaling
Cidec	Cell death-inducing DFFA-like effector c	2.24	3.34	0.76	PPARγ signaling
S3–12	Plasma membrane associated protein, S3–12	1.59	1.71	0.78	PPARγ signaling, adipocyte